Available online at www.sciencedirect.com
SCIENCE DIRECT®
Nuclear Instruments and Methods in Physics Research B 207 (2003) 291–295
NIM B Beam Interactions with Materials & Atoms
www.elsevier.com/locate/nimb

Low current MeV Au^{2+} ion-induced amorphization in silicon: Rutherford backscattering spectrometry and transmission electron microscopy study

J. Kamila [1], B. Satpati, D.K. Goswami, M. Rundhe, B.N. Dev, P.V. Satyam *

Institute of Physics, Sachivalaya Marg, Bhubaneswar 751 005, India

Received 14 November 2002; received in revised form 2 January 2003

Abstract

The amorphization due to MeV Au^{2+} ion implantation in Si(1 1 1) has been studied using Rutherford backscattering spectrometry/channeling (RBS/C) and transmission electron microscopy (TEM) methods. 1.5 MeV Au^{2+} ions were implanted into Si(1 1 1) substrates at various fluences at low currents (0.02–0.04 $\mu A\,cm^{-2}$) while the samples were kept at room temperature. The RBS/C results for as-implanted specimen shows the onset fluence for amorphization to be $\approx 5 \times 10^{13}$ ions cm^{-2} which is much lower than the fluence reported earlier. Selected area diffraction (TEM) for a sample implanted at a of 1×10^{14} ions cm^{-2} confirms the occurrence of the amorphization. Earlier, amorphization studies by Alford and Theodore, using 2.4 MeV gold ions in silicon (1 0 0) reported a threshold fluence of 1.8×10^{15} ions cm^{-2} for amorphization when the implantation was carried out at higher currents (0.2–5 $\mu A\,cm^{-2}$) [J. Appl. Phys. 76 (1994) 7265]. The nuclear energy loss (S_n) for 1.5 MeV gold ions in silicon is $\approx 13\%$ greater than the value for 2.4 MeV and cannot be the sole reason for lower threshold fluence for the amorphization. The amorphization at a relatively lower fluence for the low current implantations could be possible due to reduction in the dynamical annealing effects.

PACS: 61.80.Jh; 61.18.Bn; 61.14.Lj
Keywords: MeV ion implantation; Amorphization; Dynamical annealing; Surface and interfaces

1. Introduction

Ion implantation has been extensively used to obtain a wide variation in near-surface microstructure and properties. Using MeV ions it has become possible to make structures of interest such as buried conducting layers [1] and very large scale integration (VLSI) deep wells [1,2]. The damage produced during MeV ion implantation can be used to reduce minority carrier life time in Si and to provide buried gettering sites for collection of metallic impurities [3]. Energetic ions induce damage in the silicon and at higher fluences, a phase transformation from crystalline Si (c-Si) to amorphous Si (a-Si) can occur. Damage induced by ion irradiation in Si depends on fluence, flux,

* Corresponding author. Tel.: +91-674-2301058; fax: +91-674-2300142.
E-mail address: satyam@iopb.res.in (P.V. Satyam).
[1] Present address: B.J.B. College, Bhubaneswar, India.

0168-583X/03/$ - see front matter
doi:10.1016/S0168-583X(03)00459-2

energy of the ion, mass of the ion, target temperature, tilt angle of the target, etc. [4,5]. Understanding the amorphization process is still an active area of research and various mechanisms have been put forward [6–10]. A few decades ago, Morehead and Crowder proposed that the amorphization initially occurs in the cylindrical region around each ion path [6] and a continuous amporphization can be explained assuming that there will be sufficient overlap of the amorphized cylindrical cascades and this mechanism was known as heterogeneous amorphization. Swanson et al. [7] and Holland et al. [8] introduced a homogeneous model according to which amorphization was a phase transition induced by an accumulation of sufficient number of defects in crystalline silicon [9].

Previous studies using MeV Au ion implantation in silicon dealt with determination of range, straggling and lateral spread of Au ions as a function of energy, incident angle and temperature [10–12]. The values of measured projected range (R_p) and the straggling of MeV Au ions in silicon were found to be consistently larger than the values predicted by TRIM [13] for both the low current implantation (0.02–0.04 $\mu A\,cm^{-2}$) [11] and high current implantation (0.5–2.0 $\mu A\,cm^{-2}$) [4]. In the present work, we report the study of amorphization caused by 1.5 MeV Au^{2+} ion implantation in Si(1 1 1) single crystals at various fluences and at low currents while the substrate was kept at room temperature. Low current implantation was chosen to avoid dynamic annealing of damage. To our knowledge, the onset fluence for amorphization in case of low current ($\approx$0.02 $\mu A\,cm^{-2}$) MeV Au ion implantation in silicon has not been addressed. The onset fluence of amorphization for the high current 2.4 MeV Au-ion implantation into Si(1 0 0) was found to be $\approx 1.8 \times 10^{15}$ ions cm^{-2} [4].

2. Experimental details

Implantations were carried out with 1.5 MeV Au^{2+} ions into silicon single crystals. Prior to the implantation, the mirror polished (1 1 1)-oriented Si single crystals (type N, $\rho \sim 0.5$–30 $\Omega\,cm$) were cleaned (rinsed) with de-ionized water followed by rinsing in methanol, trichloroethelene, methanol and a final rinse in de-ionized water. The native oxide was not etched. All the implantations were performed at room temperature at the ion-implantation beam line at the 3.0 MV tandem Pelletron accelerator [14]. The implantation beam line has a raster scanner to scan the beam on the sample for providing uniform implantation over a predefined area. The implantation was performed at an angle of 5° between the sample surface normal and the incident ion beam in an attempt to minimize channeling effects during the implantation [15]. The incident ion current was kept between 0.02 and 0.04 $\mu A\,cm^{-2}$. The total fluence on the samples varied from 1×10^{13} to 1×10^{15} ions cm^{-2}. The Rutherford backscattering spectrometry/channeling (RBS/C) measurements were carried out using the above mentioned accelerator facility with 2.0 MeV He^{2+} ions. Planar and cross-section transmission electron microscopy (TEM) measurements were carried out with 200 keV electrons (2010 UHR JEOL) at our Institute [16].

3. Results and discussion

We report the fluence dependence of amorphization studies of 1.5 MeV Au^{2+} ion-implanted Si(1 1 1) single crystals using RBS/C and X-TEM methods. Fig. 1 shows the random and aligned RBS spectra from Si-single crystal specimens implanted with 1.5 MeV Au^{2+} ions at different fluences (1×10^{13}–1×10^{15} ions cm^{-2}). The onset fluence for amorphization can be observed at 5×10^{13} ions cm^{-2}. The amorphous layer for 1×10^{15} ions cm^{-2} fluence starts very close to the surface and has a width of ~445 nm. For 10^{14} ions cm^{-2} fluence the amorphous layer width is ~382 nm and that for the 5×10^{13} cm^{-2} fluence is ~150 nm. The measured amorphized layer width for the case of 5×10^{13} ions cm^{-2} fluence could be actually smaller as the backscattered yield in RBS/C measurements is affected by dechanneling of incident ions. The planar TEM measurements on this sample (data not shown) show the presence of

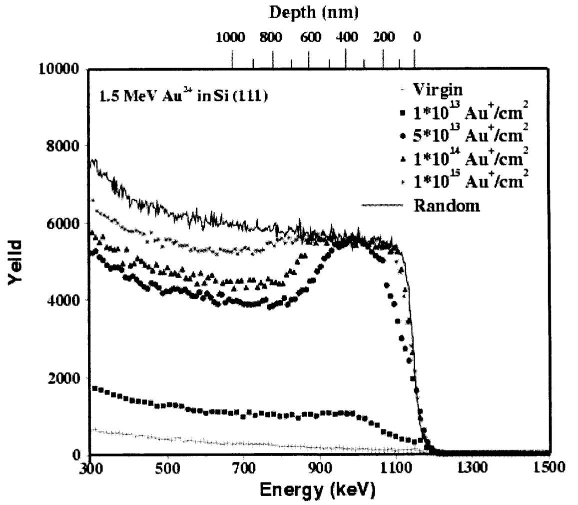

Fig. 1. 2.0 MeV He^{2+} RBS/C spectrum for 1.5 MeV Au-implanted Si(1 1 1) for as-implanted specimens at different fluences. The implantation was performed at a tilt angle of 5°. Onset of amorphization can be observed at a fluence of 5×10^{13} ions cm^{-2}. The depth scale is shown at the top.

weak amorphous rings along with the crystalline diffraction pattern.

The width of the amorphous layer was determined by converting the energy of the backscattered ions in the RBS/C spectra to a depth scale. For this purpose one needs to know the stopping cross section of He^+ ions under aligned condition. It is to be noted that the value of stopping cross section under aligned condition is smaller than that under random incidence condition. According to Kido and Kawamoto [17] the value of the stopping power for a perfect crystal under aligned condition is 0.8–0.85 times of normal stopping power. The stopping power in an aligned condition in a damaged crystal is given by

$$\varepsilon_{\text{aligned}} = (1 - f_{\text{d}})\varepsilon_{\text{virgin}} + f_{\text{d}}\varepsilon_{\text{random}},$$

where $\varepsilon_{\text{virgin}}$ is the stopping power under aligned condition in a perfect crystal and $\varepsilon_{\text{random}}$ is the stopping power of the ions under random incidence conditions, f_{d} is the dechanneling factor. We have used an RBS simulation program [18] to convert the energy to depth scale by assuming, for the aligned condition, a stopping power of $0.8 \times \varepsilon_{\text{random}}$ along the incident direction and $\varepsilon_{\text{random}}$ along the outgoing ion path. The depth scale is shown in Fig. 1. In Fig. 1, the backscattering signal from gold is not shown. The range and the straggling were determined by simulating the backscattering spectrum with GISA [19] for the as-implanted sample with the highest fluence. The experimental value of the range was found to be 420 nm and that with TRIM [13] calculation the value was found to be 385 nm. It is known that TRIM calculations underestimate the range and straggling values and our experimental results follow the previous experimental observations [4,10–12]. The onset of amorphization occurs at depth of ≈400 nm (Fig. 1, at a fluence of 5.0×10^{13} ions cm^{-2}). This correlates well with a value where Au has maximum nuclear stopping as obtained from the experimental value and with TRIM calculated value of range.

Fig. 2 shows a cross-sectional TEM micrograph (bright field) and selected area diffraction patterns (SAD) from various regions of the as-implanted sample for the fluence of 1×10^{14} ions cm^{-2}. The regions are depicted in Fig. 2(A) from which the SAD patterns were obtained. In Fig. 2(A), region (a) is near the surface, (b) is in between the surface and the amorphized region, (c) the amorphization region and region (d) corresponds to projected range of the gold ions. The SAD pattern shown in Fig. 2(c), confirms the amorphization.

Alford and Theodore [4], using 2.4 MeV gold ions in silicon (1 0 0) reported a threshold fluence of 1.8×10^{15} ions cm^{-2} for amorphization whereas we observe a fluence of 5.0×10^{13} ions cm^{-2}. This threshold fluence reduction by a factor of 36 can be understood by taking nuclear energy loss and dynamical annealing effects into account. The nuclear energy loss (S_n) for 1.5 MeV gold ions in silicon is ≈ 269 eV/Å and that for 2.4 MeV is ≈ 234 eV/Å. These values are obtained using TRIM [13]. The higher value of S_n at 1.5 MeV (≈13% higher than at value at 2.4 MeV as mentioned earlier) contributes towards the damage and hence in the amorphization process. However, this cannot be the sole cause as the reduction in the threshold fluence is about a factor of 36. At lower current implantations, the effect of dynamical

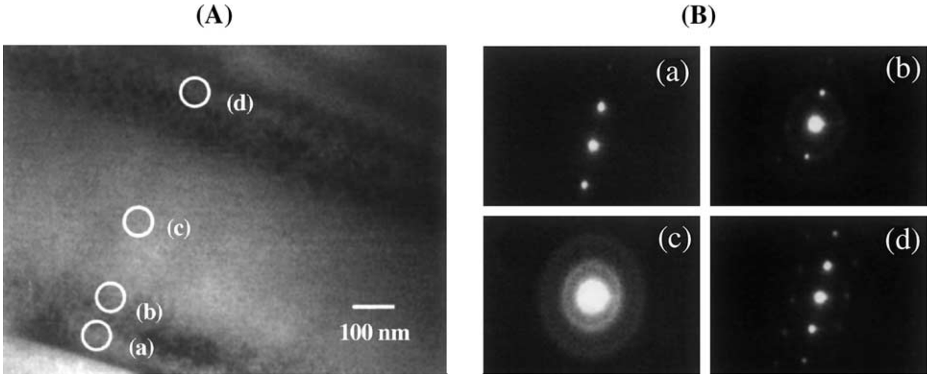

Fig. 2. (A) A cross-sectional TEM micrograph (bright field) from the implanted sample with 1×10^{14} ions cm^{-2} fluence. (B) SAD patterns from regions depicted in Fig. 2(A). Region (a) in (A) is near the surface and (a) → (d) correspond to increasing depths, depth of (d) being that of the projected range of the gold ions.

annealing is reduced and this causes a lowering of the threshold fluence for amorphization. We propose that the amorphization at a relatively lower fluence for low currents could be due to a reduction in the dynamical annealing effects.

4. Conclusions

In summary, the amorphization due to MeV Au^{2+} ion implantation in Si(1 1 1) is reported. The RBS/C results for as-implanted specimen shows the onset of amorphization to be $\approx 5 \times 10^{13}$ ions cm^{-2} which is much lower fluence than that was reported. Selected area diffraction (TEM) for a sample implanted at 1×10^{14} ions cm^{-2} confirms the occurrence of amorphization. Low current ion implantation requires lower threshold fluence for amorphization due to reduction in the dynamical annealing effects compared to high current ion implantation.

Acknowledgements

We thank Mr. A.K. Dash for help in the TEM specimen preparation. We also thank the staff at Ion Beam Laboratory, Institute of Physics, Bhubaneswar, India for their help during the implantations and RBS/C measurements.

References

[1] N.W. Cheung, C.L. Liang, B.K. Liew, R.H. Mutikainen, H. Wong, Nucl. Instr. and Meth. B 37–38 (1989) 941.
[2] A.G. Lewis, R.A. Martin, T.-Y. Huang, J.Y. Chen, M. Koyanagi, IEEE Trans. Electron. Dev. ED-34 (1987) 2156.
[3] J.M. Poate, F. Priolo, D.C. Jacobson, J.L. Batstone, M.O. Thompson, Nucl. Instr. and Meth. B 37–38 (1989) 955.
[4] T.L. Alford, N. David Theodore, J. Appl. Phys. 76 (1994) 7265.
[5] T.L. Alford, N.D. Theodore, E.L. Fleischer, J.W. Mayer, C.B. Carter, P. Borgesen, B.M. Ullrich, N.W. Cheung, H. Wong, Appl. Phys. Lett. 56 (1990) 1796.
[6] F.F. Morehead Jr., B.L. Crowder, Radiat. Eff. 6 (1970) 27.
[7] M.L. Swanson, J.R. Parsons, C.W. Hoelke, Radiat. Eff. 9 (1971) 249.
[8] O.W. Holland, S.J. Pennycook, G.L. Albert, Appl. Phys. Lett. 55 (1989) 2503.
[9] T. Motoka, S. Harada, M. Ishimaru, Phys. Rev. Lett. 78 (1997) 2980.
[10] K.-M. Wang, F. Chen, H. Hu, J.-H. Zhang, X.-D. Liu, D.-Y. Shen, T. Narusawa, M. Nagaki, Jpn. J. Appl. Phys. 41 (2002) 918.
[11] G. Kuri, Nucl. Instr. and Meth. B 117 (1996) 213.
[12] G. Kuri, B. Sundaravel, B. Rout, D.P. Mahapatra, B.N. Dev, Nucl. Instr. and Meth. B 111 (1996) 234.
[13] J.B. Biersack, L.G. Haggmark, Nucl. Instr. and Meth. 174 (1980) 257.
[14] K. Sekar, P.V. Satyam, G. Kuri, D.P. Mahapatra, B.N. Dev, Nucl. Instr. and Meth. B 73 (1993) 63.

[15] J.W. Mayer, L. Eriksson, J.A. Davies, Ion Implantation in Semiconductors (Silicon and Germanium), Academic, New York, 1970.
[16] P.V. Satyam, J. Kamila, S. Mahapatra, B. Satpati, D.K. Goswami, B.N. Dev, R.E. Cook, L. Assoufid, J. Wang, N.C. Mishra, J. Appl. Phys., submitted for publication.
[17] Y. Kido, J. Kawamoto, J. Appl. Phys. 61 (1987) 956.
[18] G. Kuri, K. Sekar, P.V. Satyam, D.P. Mahapatra, B.N. Dev, Ind. J. Phys. 70A (1996) 465.
[19] J. Saarilahti, E. Rauhala, Nucl. Instr. and Meth. B 64 (1992) 734.